

Raman Study of CVD Graphene Irradiated by Swift Heavy IonsE.A. Kolesov¹, M.S. Tivanov^{1,*}, O.V. Korolik¹, P. Yu. Apel^{2,3}, V.A. Skuratov^{2,3,4}, A.M. Saad⁵,
I.V. Komissarov⁶, A. Swic⁷, P.V. Żukowski⁸, T.N. Koltunowicz^{8,†}¹ *Belarusian State University, 4, Nezavisimosti Ave., 220030 Minsk, Belarus*² *Joint Institute for Nuclear Research, 6, Joliot-Curie, 141980 Dubna, Russia*³ *Dubna State University, 141980 Dubna, Russia*⁴ *National Research Nuclear University MEPhI, Moscow, Russia*⁵ *Al-Balqa Applied University, PO Box 4545, 11953 Amman, Jordan*⁶ *Belarusian State University of Informatics and Radioelectronics, 6, P. Brovka Str., 220013 Minsk, Belarus*⁷ *Institute of Technological Systems of Information, Lublin University of Technology, 20-618 Lublin, Poland*⁸ *Department of Electrical Devices and High Voltage Technology, Lublin University of Technology, 20-618 Lublin, Poland*

(Received 28 February 2017; revised manuscript received 19 March 2017; published online 30 June 2017)

CVD-graphene on silicon was irradiated by accelerated heavy ions (Xe, 160 MeV, fluence of 10^{11} cm⁻²) and characterized by Raman spectroscopy. The defectiveness of pristine graphene was found to be dominated by grain boundaries while after irradiation it was determined by both grain boundaries and vacancies. Respectively, average inter-defect distance decreased from ~ 24 to ~ 13 nm. Calculations showed that the ion irradiation resulted in a decrease in charge carrier mobility from $\sim 4.0 \times 10^3$ to $\sim 1.3 \cdot 10^3$ cm²/V s.

The results of the present study can be used to control graphene structure, especially vacancies concentration, and charge carrier mobility.

Keywords: Irradiated graphene, Defects, Raman spectroscopy, CVD, Swift heavy ions.

DOI: [10.21272/jnep.9\(3\).03020](https://doi.org/10.21272/jnep.9(3).03020)PACS numbers: 81.05.ue, 61.48.Gh,
78.30.Ly, 61.80. – x**1. INTRODUCTION**

Graphene is a promising material for a variety of applications. It is a two-dimensional sp²-carbon allotrope [1]. The importance of graphene studies is driven by its unique physical properties: optical transparency, high values of rigidity, thermal and electrical conductivity [2]. At present, graphene is used in transparent electrodes, field effect transistors, biosensors, etc.

For several applications, graphene structure modification using controlled defect introduction is needed [3]. Swift heavy ions (SHI) irradiation method is a versatile and convenient tool for this purpose [4]. It allows one to create defects using a wide ion energy range, different fluences for obtaining different defect densities, and various ion types. However, the mechanism of defect formation in SHI-irradiated graphene is still unclear.

Raman spectroscopy is a versatile tool for obtaining information on structural properties of various materials. This method is particularly useful in the context of graphene studies, due to monoatomic thickness of the material [1, 2]. As shown in [5], it is possible to determine the average inter-defect distance in laser spot area for graphene from *D* and *G* peaks maximum intensity ratio. Moreover, the correlation presented in [6] allows one to estimate graphene charge carrier mobility from the full width at half-maximum (FWHM) of *2D* peak.

Purpose of the present work is to study structural properties of SHI-irradiated graphene using Raman

spectroscopy in order to understand how defect-caused structural changes influence graphene physical properties.

2. EXPERIMENTAL

Graphene studied in this paper was obtained by atmospheric pressure chemical vapor deposition (CVD). Prior to the synthesis, copper substrate was electrochemically polished in 1 M phosphoric acid solution for 5 min with operating voltage of 2.3 V. Synthesis was performed in a tubular quartz reactor with a diameter of 14 mm. Copper foil was pre-annealed at 1050°C for 60 min under the following gas flow rates: hydrogen 150 cc/min, nitrogen 100 cc/min. Synthesis was performed under the following conditions: reactor temperature 1050 °C, C₁₀H₂₂ flow rate 4 μl/min, H₂ flow rate 60 cc/min, N₂ carrier flow rate 100 cc/min, synthesis time 30 min. After the hydrocarbon flow termination, the sample was cooled down to room temperature at a rate of ~ 50 °C/min.

Graphene was transferred to Si/SiO₂ substrate by wet-chemical room-temperature etching without polymer support in two steps. First, one side of copper foil was treated for 3 min in a solution of H₂NO₃ and H₂O mixed in a volume ratio of 1:3. Then the copper foil was totally dissolved in a water solution of FeCl₃. Graphene film was washed several times in a bath with distilled water prior to being placed onto the substrate.

Graphene was irradiated by 160 MeV xenon ions with total fluence of 10^{11} cm⁻² at the IC100 cyclotron at the FLNR JINR in Dubna [7]. Ion beam homogeneity

* tivanov@bsu.by† t.koltunowicz@pollub.pl

over the irradiated specimen surface was controlled using beam scanning in the horizontal and vertical directions and was better than 5 %.

Raman spectra were obtained with a spectral resolution not less than 3 cm^{-1} using a confocal Raman spectrometer Nanofinder HE (LOTIS TII). For excitation of Raman radiation, a continuous wave solid-state laser with a wavelength of 473 nm was used. Room-temperature Raman measurements were carried out using laser power of $800 \mu\text{W}$, the diameter of laser

spot on the sample surface being about $0.6 \mu\text{m}$.

3. RESULTS AND DISCUSSION

Typical Raman spectra for graphene before and after SHI irradiation are presented in Fig. 1. The presence of single-layer graphene in both cases is indicated by I2D/IG peak intensity ratios together with 2D peak FWHMs and single Lorentzian approximations (insets in Fig. 1) [2, 8].

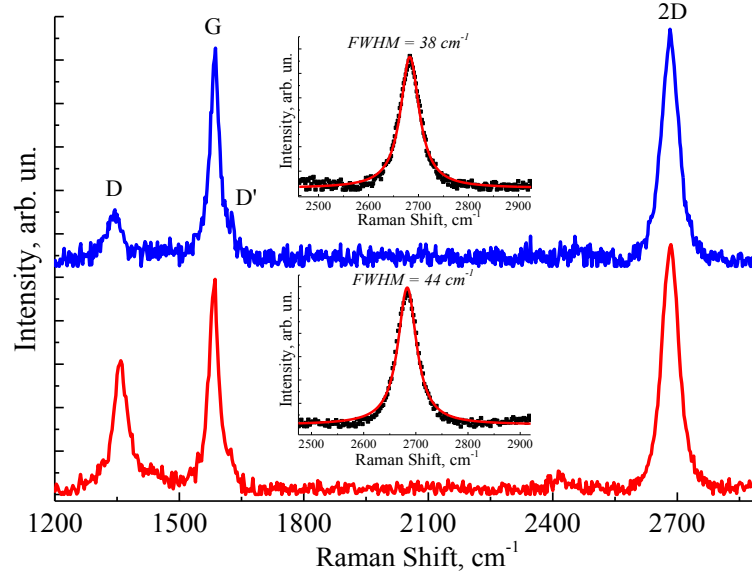


Fig. 1 – Typical Raman spectra for graphene before (top) and after (bottom) ion irradiation. Insets: 2D peak approximations with single Lorentz functions

As seen from the figure, *D* peak in pristine graphene spectrum has relatively low intensity ($I_D/I_G \sim 0.3$), which corresponds to a low defectiveness of the sample structure [1, 2]. A different situation is observed for irradiated graphene: typical Raman spectra in this case demonstrate I_D/I_G intensity ratios not less than ~ 0.5 . However, in several areas I_D/I_G values up to of ~ 1.0 are observed. Based on this fact, we can conclude that graphene defectiveness increased after irradiation.

According to [5], the average inter-defect distance in the laser spot area L_D can be calculated from the ratio of *D* and *G* peak maximum intensities using the following expression:

$$L_D^2 (nm)^2 = \frac{4.3 \cdot 10^3}{E_L^4 (eV)^4} \left(\frac{I(D)}{I(G)} \right)^{-1}, \quad (3.1)$$

where E_L is an excitation energy.

It is important to note that since the I_D/I_G ratio does not depend on a defect geometry [9], L_D values calculated from the formula represent the average inter-defect distance for all Raman active defects that are involved in elastic scattering (since the process leading to *D* peak arising includes inelastic electron-phonon scattering and elastic electron-defect scattering events [2]).

The calculation results were averaged over all obtained spectra (400 spectra for each sample). For pristine graphene, the obtained inter-defect distance

value was $\sim 24 \text{ nm}$. The calculation has shown that after the irradiation the L_D value decreased to $\sim 13 \text{ nm}$, signifying the increased number of defects. At the same time, calculated average distance between the ions fallen onto graphene surface is $\sim 16 \text{ nm}$.

In order to obtain detailed information on defect distribution over graphene surface before and after the irradiation, Raman mappings across the surface were performed. Fig. 2 presents L_D maps for graphene both before and after the irradiation.

As seen from Fig. 2, the distribution of L_D is regular over all scanned area both for pristine and irradiated graphene. The inter-defect distance uniformly decreased (and therefore the defect density increased) after the irradiation.

In [9] it was shown that graphene defect type can be obtained from $I_D/I_{D'}$ intensity ratio. *D'* peak for graphene is usually partially overlapped with *G* peak leading to combined asymmetric shape, as can be observed in Fig. 1, but its intensity can be easily obtained by simple deconvolution. Typical spectra of pristine graphene demonstrate $I_D/I_{D'}$ values of 1.0 - 3.5 corresponding to grain boundaries. At the same time, irradiated graphene spectroscopy data shows $I_D/I_{D'} \sim 3.9 - 5.7$. According to presented in [9] dependencies, these values indicate presence of both grain boundaries and vacancies.

Fig. 3 shows Raman maps of the $I_D/I_{D'}$ intensity ratio giving the distribution of defect types over the scanned area.

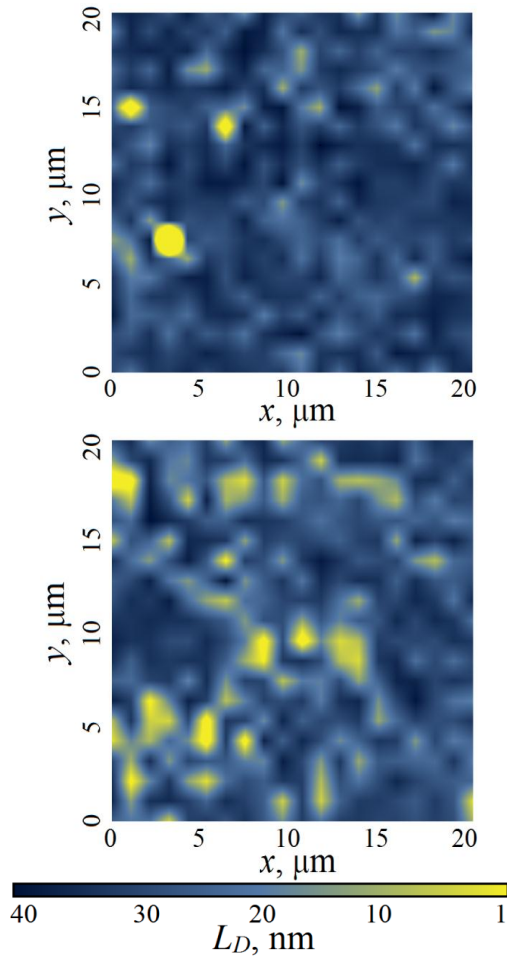


Fig. 2 – Raman maps ($20 \times 20 \mu\text{m}$) of the average inter-defect distance for pristine (top) and irradiated (bottom) graphene; scanning step of $1 \mu\text{m}$

It is seen from the figure that scanned pristine graphene area is dominated by grain boundaries. In turn, irradiated graphene map contains a large number of vacancies besides the boundaries. Moreover, Raman maps of L_D and I_D/I_D' for irradiated graphene show a very strong correlation, giving almost identical values distribution. This fact indicates that nearly all defects in this case are represented by vacancies induced during the irradiation.

According to [6], charge carrier mobility μ in graphene can be determined from $2D$ peak full width at half-maximum (FWHM). The authors of [6] used combined Hall effect measurements and Raman spectroscopy. This method resulted in finding strong correlation between Hall mobility and $2D$ peak FWHM. Determination performed according to dependencies described in [6] gave the value of charge carrier mobility in pristine graphene averaged over all 400 scanned spectra $\mu_{pr} \sim 4.0 \cdot 10^3 \text{ cm}^2/\text{V s}$. For irradiated graphene, the average μ_{irr} was about $1.3 \cdot 10^3 \text{ cm}^2/\text{V s}$. The charge carrier mobility decrease after the irradiation can be explained by intensifying of charge carriers scattering by defects induced.

4. CONCLUSION

Raman studies of CVD-graphene on silicon substrate

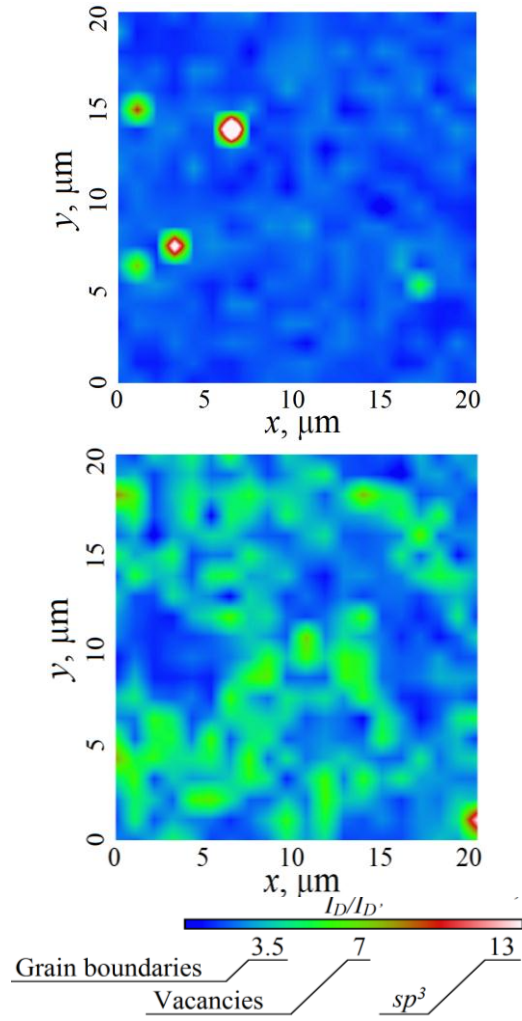


Fig. 3 – Raman maps ($20 \times 20 \mu\text{m}$) of the I_D/I_D' intensity ratio for pristine (top) and irradiated (bottom) graphene; scanning step of $1 \mu\text{m}$. Types of defects corresponding to specific I_D/I_D' values are indicated under the scale

substrate irradiated by accelerated heavy ions (Xe, 160 Me V, fluence 10^{11} cm^{-2}) have shown the uniform distribution of defect types and inter-defect distances over graphene surface. The defectiveness of pristine graphene was dominated by grain boundaries while after irradiation it became determined by both grain boundaries and vacancies. The average inter-defect distance was found to decrease from ~ 24 to ~ 13 nm. Charge carrier mobilities in graphene before and after the ion irradiation were calculated. It was found that the irradiation resulted in a decrease of charge carrier mobility from $\sim 4.0 \cdot 10^3$ to $\sim 1.3 \cdot 10^3 \text{ cm}^2/\text{V s}$. The results of the present study can be used to control graphene structure, especially vacancies concentration, and charge carrier mobility.

ACKNOWLEDGEMENTS

This work was partly supported by the statute tasks of the Lublin University of Technology, at the Faculty of Electrical Engineering and Computer Science, (S-28/E/2017), entitled “Researches of electrical, magnetic, thermal and mechanical properties of modern electrotechnical and electronic materials,

including nanomaterials and electrical devices and their components, in order to determination of

suitability for use in electrical engineering and to increase the efficiency of energy management”.

REFERENCES

1. A.C. Ferrari, J.C. Meyer, V. Scardaci, C. Casiraghi, M. Lazzeri, F. Mauri, S. Piscanec, D. Jiang, K.S. Novoselov, S. Roth, A.K. Geim, *Phys. Rev. Lett.* **97**, 187401 (2006).
2. A.C. Ferrari, D.M. Basko, *Nature Nanotech.* **8**, 235 (2013).
3. A.K. Geim, *Science* **324**, 1530 (2009).
4. J. Zeng, H.J. Yao, S.X. Zhang, P.F. Zhai, J.L. Duan, Y.M. Sun, G.P. Li, J. Liu, *Nucl. Instr. Meth. Phys. Res. B* **330**, 18 (2014).
5. L.G. Cançado, A. Jorio, E.H. Martins Ferreira, F. Stavale, C.A. Achete, R.B. Capaz, M.V.O. Moutinho, A. Lombardo, T.S. Kulmala, A.C. Ferrari, *Nano Lett.* **11**, 3190 (2011).
6. J.A. Robinson, M. Wetherington, J.L. Tedesco, P.M. Campbell, X. Weng, J. Stitt, M.A. Fanton, E. Frantz, D. Snyder, B.L. Van Mil, G.G. Jernigan, R.L. Myers-Ward, C.R. Eddy Jr., D.K. Gaskill, *Nano Lett.* **9**, 2873 (2009).
7. B.N. Gikal, S.N. Dmitriev, G.G. Gul'bekyan, P.Yu. Apel', V.V. Bashevoi, S.L. Bogomolov, O.N. Borisov, V.A. Buzmakov, I.A. Ivanenko, O.M. Ivanov, N.Yu. Kazarinov, I.V. Kolesov, V.I. Mironov, A.I. Papash, S.V. Pashchenko, V.A. Skuratov, A.V. Tikhomirov, M.V. Khabarov, A.P. Cherevatenko, N.Yu. Yazvitskii, *Phys. Partic. Nucl. Lett.* **5**, 33 (2008).
8. Y. Hao, Y. Wang, L. Wang, Z. Ni, Z. Wang, R. Wang, C.K. Koo, Z. Shen, J.T.L. Thong, *Small* **6**, 195 (2010).
9. A. Eckmann, A. Felten, A. Mishchenko, L. Britnell, R. Krupke, K.S. Novoselov, C. Casiraghi, *Nano. Lett.* **12**, 3925 (2012).